

Article

Dynamics of Vegetation Greenness and Its Response to Climate Change in Xinjiang over the Past Two Decades

Jie Xue ¹, Yanyu Wang ¹, Hongfen Teng ², Nan Wang ¹, Danlu Li ¹, Jie Peng ³, Asim Biswas ⁴ and Zhou Shi ^{1,5,*}

¹ Institute of Agricultural Remote Sensing and Information Technology Application, College of Environmental and Resource Sciences, Zhejiang University, Hangzhou 310058, China; xj2019@zju.edu.cn (J.X.); wangyanyu@zju.edu.cn (Y.W.); wangnanfree@zju.edu.cn (N.W.); lidanlu@zju.edu.cn (D.L.)

² Research Center for Environmental Ecology and Engineering, Wuhan Institute of Technology, School of Environmental Ecology and Biological Engineering, 206 Guanggu 1st Road, Wuhan 430205, China; tenghongfen@163.com

³ College of Plant Sciences, Tarim University, Alar 843300, China; pjzky@163.com

⁴ School of Environmental Sciences, University of Guelph, Alexander Hall 135, 50 Stone Road East, Guelph, ON N1G 2W1, Canada; biswas@uoguelph.ca

⁵ Key Laboratory of Spectroscopy Sensing, Ministry of Agriculture, Hangzhou 310058, China

* Correspondence: shizhou@zju.edu.cn

Citation: Xue, J.; Wang, Y.; Teng, H.; Wang, N.; Li, D.; Peng, J.; Biswas, A.; Shi, Z. Dynamics of Vegetation Greenness and Its Response to Climate Change in Xinjiang over the Past Two Decades. *Remote Sens.* **2021**, *13*, 4063. <https://doi.org/10.3390/rs13204063>

Academic Editors: Christopher Post and Hamdi A. Zurqani

Received: 19 August 2021

Accepted: 08 October 2021

Published: 11 October 2021

Publisher's Note: MDPI stays neutral with regard to jurisdictional claims in published maps and institutional affiliations.



Copyright: © 2021 by the authors. Licensee MDPI, Basel, Switzerland. This article is an open access article distributed under the terms and conditions of the Creative Commons Attribution (CC BY) license (<http://creativecommons.org/licenses/by/4.0/>).

Abstract: Climate change has proven to have a profound impact on the growth of vegetation from various points of view. Understanding how vegetation changes and its response to climatic shift is of vital importance for describing their mutual relationships and projecting future land–climate interactions. Arid areas are considered to be regions that respond most strongly to climate change. Xinjiang, as a typical dryland in China, has received great attention lately for its unique ecological environment. However, comprehensive studies examining vegetation change and its driving factors across Xinjiang are rare. Here, we used the remote sensing datasets (MOD13A2 and TerraClimate) and data of meteorological stations to investigate the trends in the dynamic change in the Normalized Difference Vegetation Index (NDVI) and its response to climate change from 2000 to 2019 across Xinjiang based on the Google Earth platform. We found that the increment rates of growth-season mean and maximum NDVI were 0.0011 per year and 0.0013 per year, respectively, by averaging all of the pixels from the region. The results also showed that, compared with other land use types, cropland had the fastest greening rate, which was mainly distributed among the northern Tianshan Mountains and Southern Junggar Basin and the northern margin of the Tarim Basin. The vegetation browning areas primarily spread over the Ili River Valley where most grasslands were distributed. Moreover, there was a trend of warming and wetting across Xinjiang over the past 20 years; this was determined by analyzing the climate data. Through correlation analysis, we found that the contribution of precipitation to NDVI ($R^2 = 0.48$) was greater than that of temperature to NDVI ($R^2 = 0.42$) throughout Xinjiang. The Standardized Precipitation and Evapotranspiration Index (SPEI) was also computed to better investigate the correlation between climate change and vegetation growth in arid areas. Our results could improve the local management of dryland ecosystems and provide insights into the complex interaction between vegetation and climate change.

Keywords: arid areas; vegetation variation; climate change; MOD13A2; Google Earth Engine

1. Introduction

Vegetation performs an essential part in terrestrial ecosystems, which influence soil, the atmosphere, moisture and other natural items [1,2]. It also affects the balance of the energy of the earth–atmosphere system [3]. Therefore, vegetation and its dynamic changes have received much attention over the years [4–7]. Researching vegetation

change in dryland is now in the mainstream [8,9]. Drylands are critical global environments, accounting for around 40% of the earth's land surface and over 2×10^9 people live in these regions [10]. The types of land cover vary in arid areas and include sandy deserts, temperate grasslands, savanna woodland, etc. [11]. Because of the high sensitivity to climate in arid areas, the ecosystems of drylands are expected to have a strong response to climate change [12]. Therefore, research on drylands is critical and essential, especially for realizing the response of dryland ecosystems to climate change. Traditional vegetation monitoring methods require a lot of manpower and material resources, and the data acquisition cycle is long and the coverage area is small, making it difficult to obtain data over the large-scale. It is the appearance of remote sensing technology that has made up for the deficiencies of conventional monitoring methods. This is an excellent way to detect the dynamic changes in vegetation by remote sensing since it can acquire a wide range of data in a short time and data acquisition is convenient and free of charge.

A wide range of vegetation indices have arisen based on remote sensing [13], such as the Normalized Difference Vegetation Index (NDVI), Leaf Area Index (LAI), Enhanced Vegetation Index (EVI), etc. [14]. NDVI has been used quite extensively among the different spectral vegetation indexes retrieved from remote sensing [13,15], owing to its simplicity and robustness [16,17]. NDVI is also sensitive to canopy configurations, chemical compositions, photosynthesis, and vegetation production in sparse canopy areas [18,19]. Monitoring and assessing NDVI changes in vegetation are central to the evaluation of vegetation performance under fluctuating climate patterns and to track the quality of the ecological environment [20]. The entire phenological cycle of vegetation is most active during the growing season and is usually used to explore vegetation dynamics in this stage, other than in evergreen forests [21]. Therefore, detecting the NDVI can represent the characteristics of the changes in vegetation cover during the growing season [22].

Most current studies have indicated that a global greening trend in vegetation has occurred over the last 40 years [23]. The situation is similar in arid regions [8,24]. There are different vegetation changes in different environmental conditions, and many factors contribute to the changes in vegetation greenness. Much research has focused on the effects of several climate factors, such as precipitation, temperature and evaporation, especially in arid and semi-arid regions because of their high sensibility to climate change [25–28]. Lian et al. [8] advocated that the intensification of meteorological drought and the improvement of vegetation growth occurred simultaneously in arid regions. Nemani et al. [29] suggested that warming caused NDVI to increase in the middle latitudes of the Northern Hemisphere while temperature and precipitation both affected NDVI in arid regions.

With the accumulation of different satellite data, there are several frequently-used long time series datasets of NDVI, such as NOAA/AVHRR NDVI, SPOT-VGT NDVI, MODIS NDVI, etc. [30]. The MODIS imaging sensor started to collect in 2000, and is regarded as bringing an improvement in measuring surface condition [31]; it is widely used now in vegetation dynamics detection. MODIS is good at NDVI dynamic monitoring and the data is of low fluctuation [32]. Meanwhile, MODIS NDVI datasets are advantageous because of their high spectral resolution [33]. Furthermore, it has a greater dynamic range of NDVI than other data [34].

It is worth noting that paying attention to only one of these three factors (precipitation, temperature and evaporation) regarding their effect on vegetation changes in arid areas is one-sided [35]. Some studies have not comprehensively analyzed the factors influencing vegetation change. For example, research pointed out that warming was the dominant driver causing the acceleration of vegetation green-up from 1982 to 2016 [36]. Another study concluded that increased precipitation and irrigation practices are important reasons for greening in arid areas [9]. Standardized Precipitation and Evapotranspiration Index (SPEI) could fill this gap since it performs well over dryland [37]. Meanwhile, as a drought index, SPEI is better at evaluating the drought crises due to global warming in drylands [38]. In addition, NDVI change rates in different vegetation types

are distinguishable. However, most existing research has concentrated on the whole vegetation regardless of vegetation types, and there is a need for finer classification of vegetation to analyze its response to climate [39].

Xinjiang is a representative arid region located in northwestern China, with a proportion of about a sixth of the overall Chinese territory. It is a significant strategic region [40,41] and it is reported that the warming rate of almost 0.3 °C per decade makes the vegetation of Xinjiang sensitive to climate shift [42]. There some researchers are paying attention to the relationships between vegetation and climate factors in this area, but the results are different. Zhang et al. [43] found that the vegetation showed apparent greening trends in most parts of Xinjiang, and temperature and moisture mainly controlled this vegetation change. Luo et al. [35] explored the reasons for the significant increase in NDVI in northern Xinjiang through the lag effects of drought on vegetation, and verified the strong and positive correlation between NDVI and precipitation. Xu et al. [44] drew a conclusion that the grassland in southern Xinjiang is more sensitive to temperature change than that in northern Xinjiang. This research used either interpolated climate datasets or data from meteorological stations, but did not combine the two types of data to explore the response of NDVI to climate changes in multiple dimensions. We used the data from meteorological stations and a grid cells dataset to investigate climate change and its correlation with vegetation growth in this study.

This study was conducted to explore the NDVI dynamic change trends and their response to climate change from 2000 to 2019 across Xinjiang, relying on the Google Earth Engine (GEE) platform. Specifically, this study aimed to (1) detect the trend of NDVI change in the plant growing season in Xinjiang over the past two decades; (2) investigate the changes in vegetation greenness with different land use; (3) calculate the SPEI and analyze the influence of climate (precipitation, temperature and SPEI) changes on the dynamics of vegetation greenness. The results are promising with relation to improving the management of dryland ecosystems, delving into the response of different vegetation to climate change, and dealing with the effects of climate shift to improve the ecology.

2. Materials and Methods

2.1. Study Area

Xinjiang is situated along the northwestern border of China between 73°20′–96°25′E and 34°15′–49°10′N (Figure 1). It is a typical arid area, with a total area of approximately 1.66 million km². The three major mountain systems, Kunlun Mountains, Tianshan Mountains and Altai Mountains, which extend roughly in the zonal direction, separate the Junggar and Tarim Basins, forming a unique landscape pattern of mountains and basins [45]. There are obvious differences in the vertical zoning of the mountains. The unique topographical distribution creates in Kunlun, Tianshan and Altai Mountains a large amount of grassland and forest vegetation. Meanwhile, Junggar and Tarim Basins are covered by typical temperate desert vegetation. Oases and cities are distributed in the valley plains. Although Xinjiang belongs to a temperate continental climate, due to the large north-south span of Xinjiang, a pattern with the Tianshan Mountains as the boundary is formed, and the physical and geographical conditions of southern and northern Xinjiang are quite different. The regional climate features of drought, low rainfall, and high winds have formed a widespread desert on the Gobi landscape. The vegetation generally provides a low degree of coverage, and the ecosystem is relatively fragile and sensitive. It is an ideal area for researching vegetation changes and their correlation with climate change.

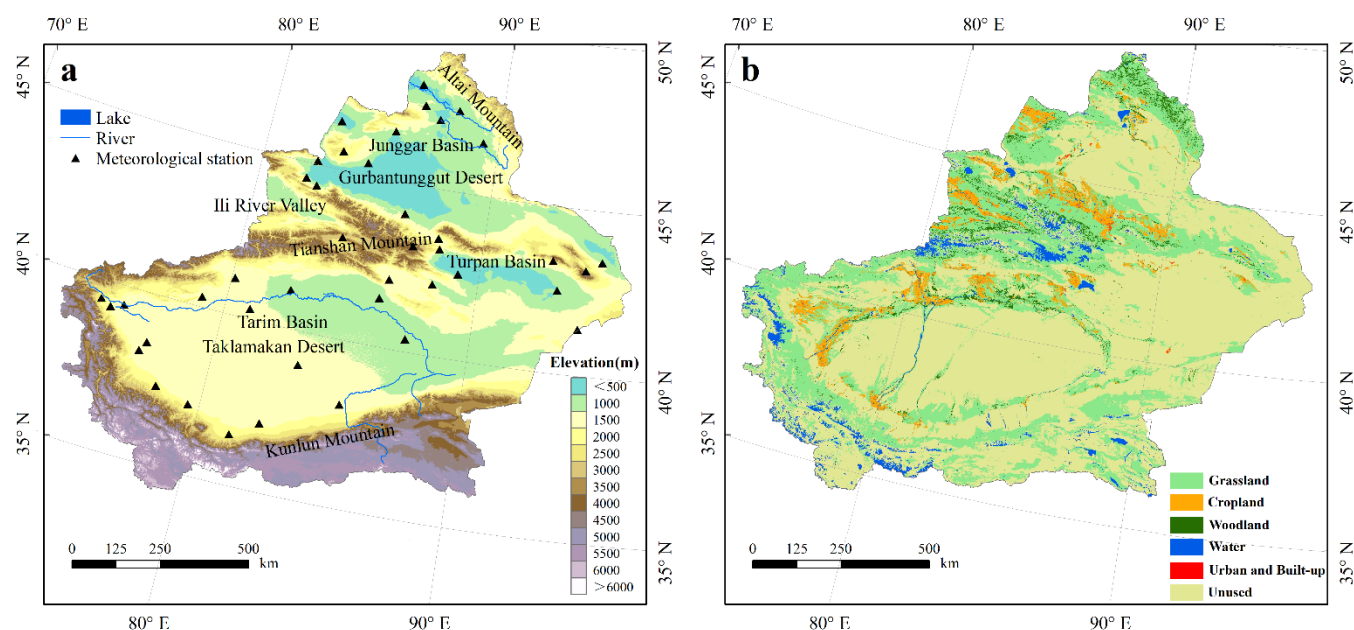


Figure 1. (a) Meteorological stations in Xinjiang overlaid on the terrain map (Shuttle Radar Topography Mission; <https://eospso.gsfc.nasa.gov/missions/shuttle-radar-topography-mission>, accessed on 8 February 2021). (b) Land use types in 2010 in Xinjiang (<http://www.resdc.cn/>, accessed on 2 March 2021).

2.2. Datasets

2.2.1. NDVI Dataset

Given the long temporal sequences of the study period and a large study area, we selected 20 years (2000–2019) of MOD13A2 NDVI data to evaluate the vegetation dynamics. The MOD13A2 dataset was a 16-day period collection at a spatial resolution of 1 km. We retrieved the NDVI data from GEE (https://developers.google.com/earth-engine/datasets/catalog/MODIS_006_MOD13A2#citations, accessed on 13 February 2021). For purpose of minimizing the effects of ice and snow, the NDVI was considered in a plant growing season which was from May to September during 2000–2019 [10]. We identified the monthly NDVI with the maximal value composites (MVC). The mean NDVI ($NDVI_{mean}$) and maximum NDVI ($NDVI_{max}$) mentioned in this study were computed on the basis of the corresponding NDVI during the plant growing season. For fear of noise from non-vegetation signals, we got rid of the time series grid cells with $NDVI_{mean}$ lower than 0.1 (2000–2019) during the plant growing seasons [46,47].

2.2.2. Climate Data

We obtained daily temperature and precipitation data from 42 meteorological stations during 2000–2018 in Xinjiang (Figure 1a). To correspond with the NDVI data, we calculated mean temperature and total precipitation for the plant growing season (May to September) from 2000 to 2018 depending on the data mentioned above.

We obtained the TerraClimate dataset from GEE (https://developers.google.com/earth-engine/datasets/catalog/IDAHO_EPSCOR_TERRACLIMATE, accessed on 13 February 2021). This dataset is a monthly climate and climatic water balance for global terrene surfaces with a high-spatial resolution of 2.5 arc min from 1958 to present [48]. To correspond with the NDVI data, we calculated the temperature and total precipitation (May to September) based on this dataset through GEE to investigate the climate change on the pixel scale during the study period (2000–2019).

To better reflect the correlation between climate shift and plant change in arid areas, we also calculated the monthly SPEI for the plant growing season through GEE based on

the TerraClimate dataset. SPEI is a drought metric based on climate data [49], which explains both temperature and precipitation influences on soil moisture; it works especially well over dryland areas [37]. Meanwhile, we also used the points data of 42 meteorological stations to extract SPEI from grid data. We calculated the SPEI using Equation (1):

$$SPEI_j = P_j - PET_j, \quad (1)$$

where p is precipitation, PET is potential evapotranspiration (gained from the Penman-Monteith approach), and j is the unit time. Here j refers to the plant growing season (May to September) from 2000–2019.

In accordance with the standards put forward by China in 2006 [50], the drought classification is divided into 8 levels with SPEI between -2 and 2 , and the corresponding levels are from extreme drought to extremely wet.

2.2.3. Land Use Data

In our research, we used the land use types of 2010 (Figure 1b) as a benchmark to analyze the NDVI changes for different vegetation types. Because 2010 is the middle year of the study period, the land use types of 2010 represent the land use types of the two decades. The land use map was developed from the Resource and Environment Data Center of the Chinese Academy of Sciences (<http://www.resdc.cn/>, accessed on 2 March 2021). There are six categories of land use type (cropland, woodland, grassland, water, urban and built-up and unused areas), among which water also includes permanent glaciers and snow [51].

We took three main land use types (woodland, grassland and cropland) in Xinjiang as the research objects and analyzed their responses to climate variation, and discussed the sensitivity of different plants to climate change in arid areas. The vegetated areas cover 35.43% of Xinjiang, of which 28.89% is grassland, 4.23% is cropland and 2.31% is woodland (Figure 2d). The unused area and other areas are sparsely vegetated or non-vegetated, and our study does not focus on these areas.

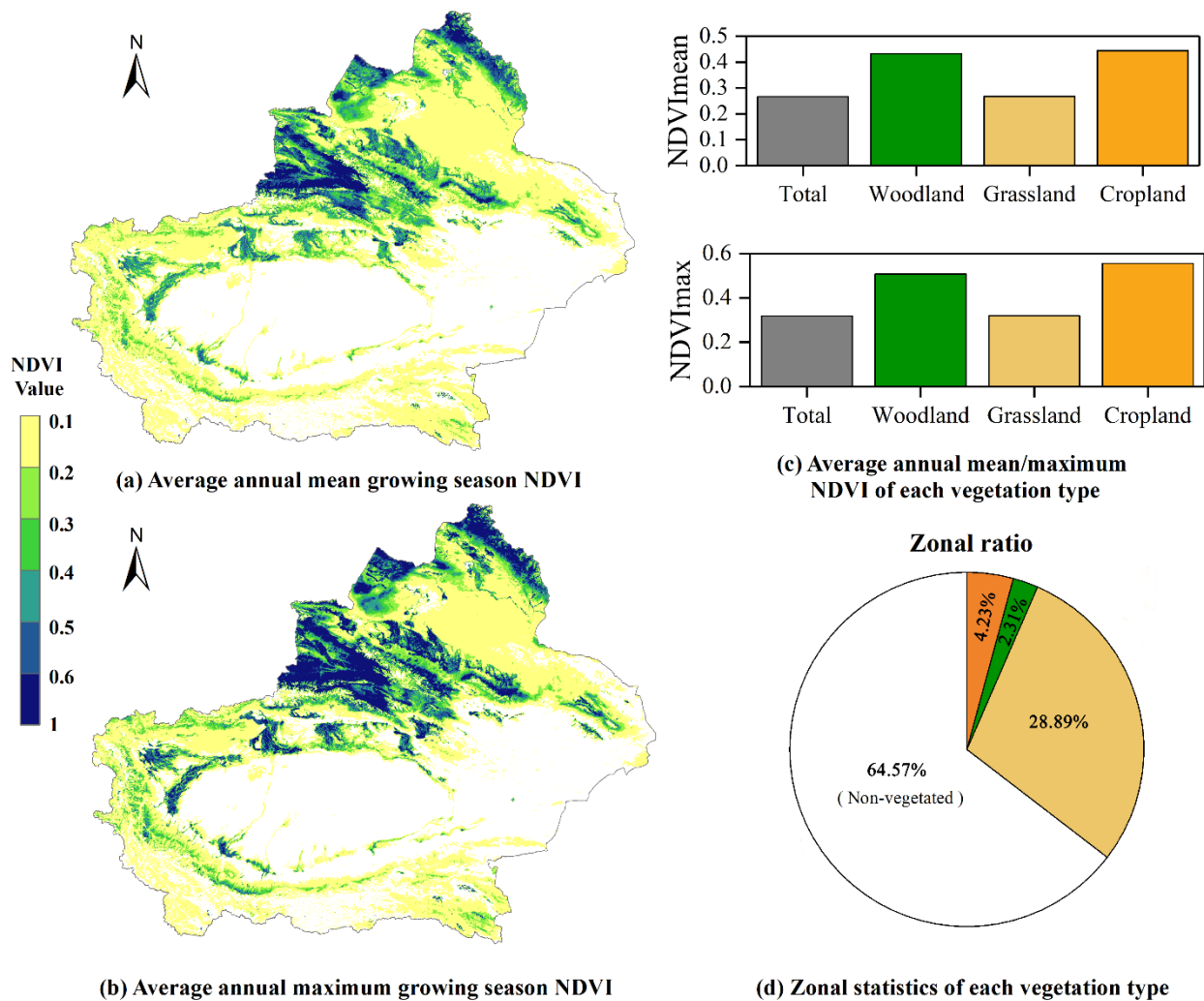


Figure 2. Spatial patterns of the long-term average growing season NDVI for 2000–2019, (a) mean NDVI ($NDVI_{mean}$), (b) maximum NDVI ($NDVI_{max}$). The white parts indicate the areas where the multiyear $NDVI_{mean}$ is under 0.1. (c) Average annual $NDVI_{mean}$ and $NDVI_{max}$ of each land use type for 2000–2019. The NDVI was calculated for the growing season from May to September. (d) Zonal statistics for each land use type were based on the land use map.

2.3. Methods

2.3.1. Spatio-Temporal Change Analysis

In this study, we applied the linear regression method based on the least squares approach to estimate the NDVI spatial change rate in the course of the plant growing season (May–September) of twenty years (2000–2019), and used the slope of the regression curve to present the change trend. We also calculated the p -value based on the F test to analyze the significance of the slope in the model, and $p < 0.05$ is a significant change [52,53]. The slope is calculated in Equation (2):

$$Slope = \frac{n \times \sum_{i=1}^n i \times NDVI_i - \sum_{i=1}^n i \sum_{i=1}^n NDVI_i}{n \times \sum_{i=1}^n i^2 - (\sum_{i=1}^n i)^2}, \quad (2)$$

where i indicates 1 for the first year (2000) of the study, 2 for the second year (2001), and so on; n equates to the summation years of the research period; and $NDVI_i$ represents the value of annual NDVI in time of the i th year. If the slope is larger than 0, the $NDVI$ increased; otherwise, it declined.

The change trend of the yearly average maximum temperature and total precipitation are the same as the NDVI.

2.3.2. Correlation Analysis

We calculated the Pearson correlation using the MATLAB software in the spatial distribution maps to uncover the correlation between NDVI and the climate dataset. This can display the positive or negative correlation between the two variables for each pixel. The R represents the Pearson correlation, which is calculated by formula (3):

$$R = \frac{\sum_{i=1}^n [(x_i - \bar{x})(y_i - \bar{y})]}{\sqrt{\sum_{i=1}^n (x_i - \bar{x})^2 \sum_{i=1}^n (y_i - \bar{y})^2}}, \quad (3)$$

where x_i and y_i mean the individual values of climate factors and NDVI for the i th year, while \bar{x} and \bar{y} are the mean of climate factors and NDVI values over 20 years.

3. Results

3.1. NDVI Dynamic Changes

3.1.1. Annual NDVI Spatial Change Trend

The change rate in Xinjiang was derived by linear regression, which is a long time series plant growing season NDVI change throughout the period from 2000 to 2019. As presented in Figure 3, the overall patterns of the change rates of mean and maximum of NDVI were positive in Xinjiang, and they had similar spatial patterns of greening (increasing tendency of NDVI) and browning (decreasing tendency of NDVI).

The greatest change rate of mean NDVI (R_{mean}) was observed among the northern Tianshan Mountains, southern Junggar Basin and northern margin of the Tarim Basin, where the main vegetation type is cropland, while the lowest R_{mean} was observed over the Ili River Valley where woodlands and grasslands were distributed. The spatial distribution of browning areas is in keeping with existing research [24,43]. The R_{mean} (Figure 3c) in Xinjiang was 0.0011 per year. The change rate of maximum NDVI (R_{max}) (Figure 3c) was 0.0013 per year in Xinjiang, and the change regions (Figure 3b) resembled that of R_{mean} , while the change degree was greater than R_{mean} . The results were relatively in accord with the results acquired by Luo et al. [35] who researched the NDVI change from 1998 to 2015 in northern Xinjiang. Jiapaer et al. [24] also observed the same vegetation dynamics in Xinjiang. From Figure 3d, we found that the greening pixels of $\text{NDVI}_{\text{mean}}$ were 95.35%, and the browning pixels were 4.65%. Meanwhile, the greening pixels of NDVI_{max} were more numerous than the browning pixels. The results suggested that the situation for plant growth is improving over time. On the whole, the results of the vegetation change in Xinjiang were similar to previous research, the minor discrepancies in results probably due to the differences in study area and period.

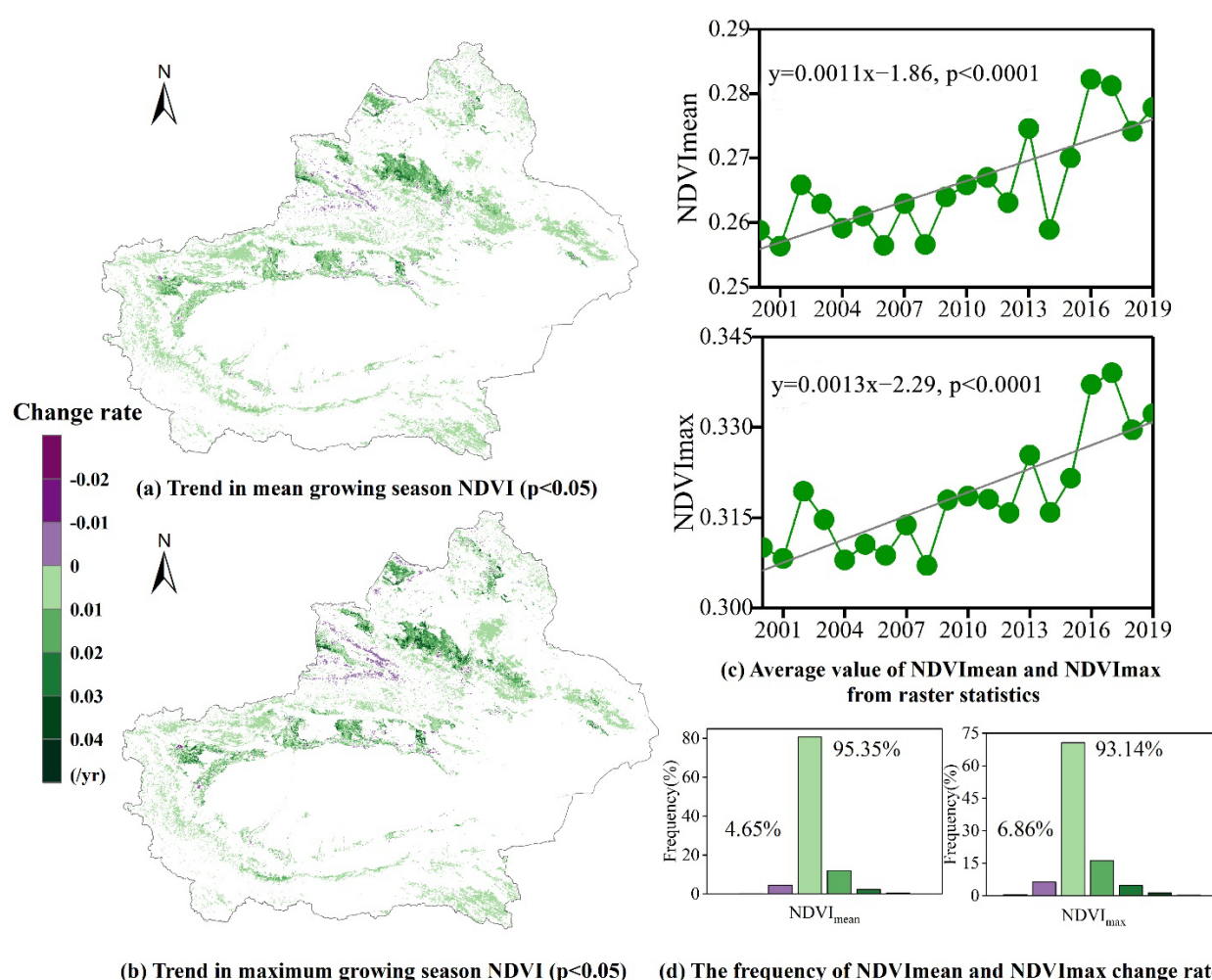


Figure 3. The spatial patterns of (a) change rate of mean NDVI (R_{mean}) for 2000–2019 and (b) change rate of maximum NDVI (R_{max}) for 2000–2019. The white parts indicate the areas where the multiyear NDVI_{mean} is under 0.1. (c) The long-term trend of NDVI_{mean} and NDVI_{max} for 2000–2019 based on the average value from zonal raster statistics. (d) The frequency of NDVI_{mean} and NDVI_{max} change rate for different numerical intervals. The NDVI was calculated throughout the growing season (May to September).

3.1.2. Annual NDVI Change for Diverse Land Use Types

Diverse land use types showed dissimilar change trends in Xinjiang, but the NDVI for all vegetation showed an upward trend over the two decades (2000–2019) (Figure 4). For example, cultivated vegetation in croplands, which has the highest value of NDVI_{mean} (0.44) and NDVI_{max} (0.56) (Figure 2), showed a significant and rapid greening rate for R_{mean} (0.0067 per year) and R_{max} (0.0077 per year) over the study period. The greening rate of R_{mean} (0.0011 per year) and R_{max} (0.0015 per year) in the grassland is lower than other land use types. The greening rates of R_{mean} (0.0014 per year) and R_{max} (0.0017 per year) in the woodland are at a moderate rate among land use types. The increasing trend of NDVI proved that the environment for vegetation growth is improving. Furthermore, the response of all vegetation to environmental changes was diverse, and the distinct change rates of the different types of vegetation demonstrated that there are many reasons behind vegetation greenness.

Viewing the segment changes of NDVI, we can find that the average and maximum values of NDVI of all three land use types have increased significantly compared to the previous year in 2005, 2007 and 2013. In contrast, a marked decline was observed in 2006, 2008, 2014 and 2018. This reflected the opposite NDVI change trends in different periods, with woodland and grassland both decreasing in 2004 and increasing in 2009. However,

the NDVI of croplands increased in 2004 and decreased in 2009. These results indicated that the responses to environmental change of the natural vegetation are different than artificial cultivation vegetation.

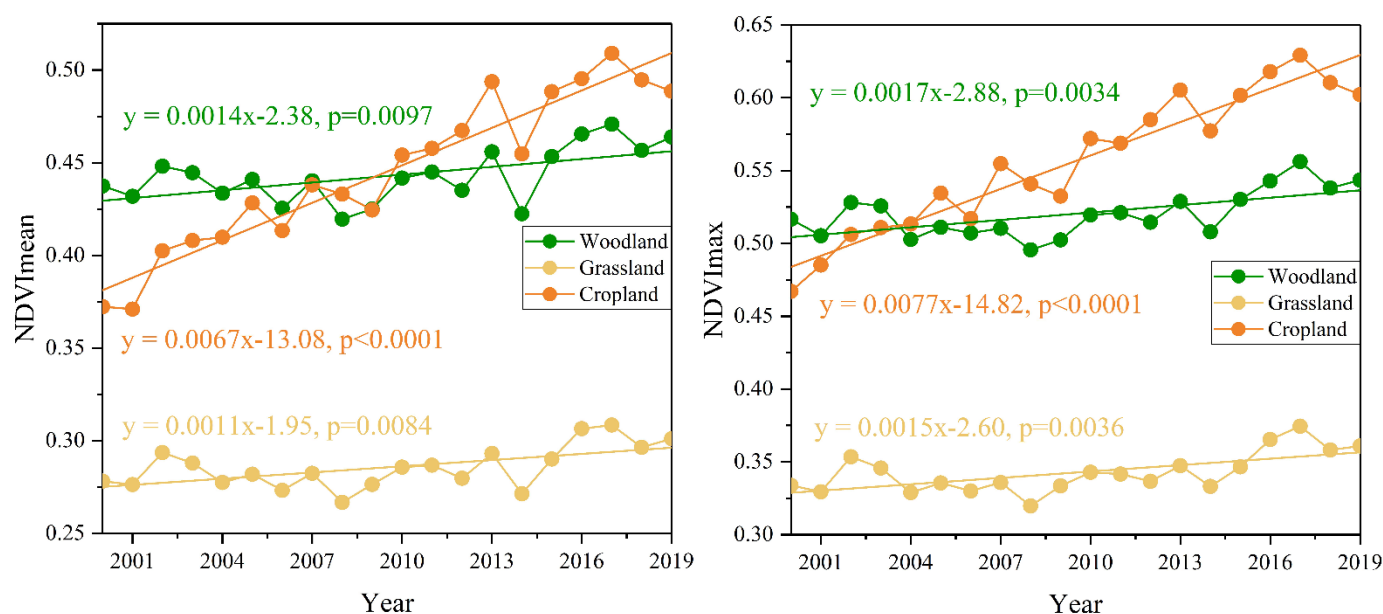


Figure 4. The average NDVI_{mean} and NDVI_{max} of the grid cells for every land use type in plant growing season for two decades (2000–2019).

3.2. Climate Change

The changes in total precipitation, average temperature and SPEI during the long-term growth season (May–September) based on meteorological stations are shown in Figure 5. This shows that the total precipitation, mean temperature and SPEI were increasing. Across Xinjiang, the change rate of total precipitation was 0.994 per year, average temperature was 0.028 per year and the average SPEI was 0.046 per year. Among the three types of land use, cropland experienced the greatest change in precipitation (1.84 per year), grassland has the largest change in temperature (0.034 per year), and woodland has the largest change in SPEI (0.119 per year). Meanwhile, temperature (0.028 per year) and SPEI (0.031 per year) have the least change in cropland, and precipitation has the least change in grassland (1.11 per year). The higher the SPEI, the lighter the drought occurrence. The results indicated that there has been a trend of warming and increased humidity across Xinjiang over the past 20 years.

Except for cropland, the average temperature was relatively low in 2003, 2009, 2013 and 2017, and the corresponding total precipitation was relatively high. At the same time, evaporation was often relatively low, and the corresponding SPEI was relatively high. Compared with the above years, opposite results were obtained in 2001, 2008, and 2014. It is reported that Xinjiang suffered from heavy drought in 2008 and 2014 [54,55], therefore the SPEI in these years were very low. As for cropland, the average temperature was relatively low in 2004, 2010, 2012, and 2017 whereas the mean total precipitation and SPEI were relatively high for the latter three years. In 2001, 2008, and 2011 the average temperature was relatively high. SPEI is correlated with precipitation and temperature. In grassland, SPEI reflects the high and low values of precipitation.

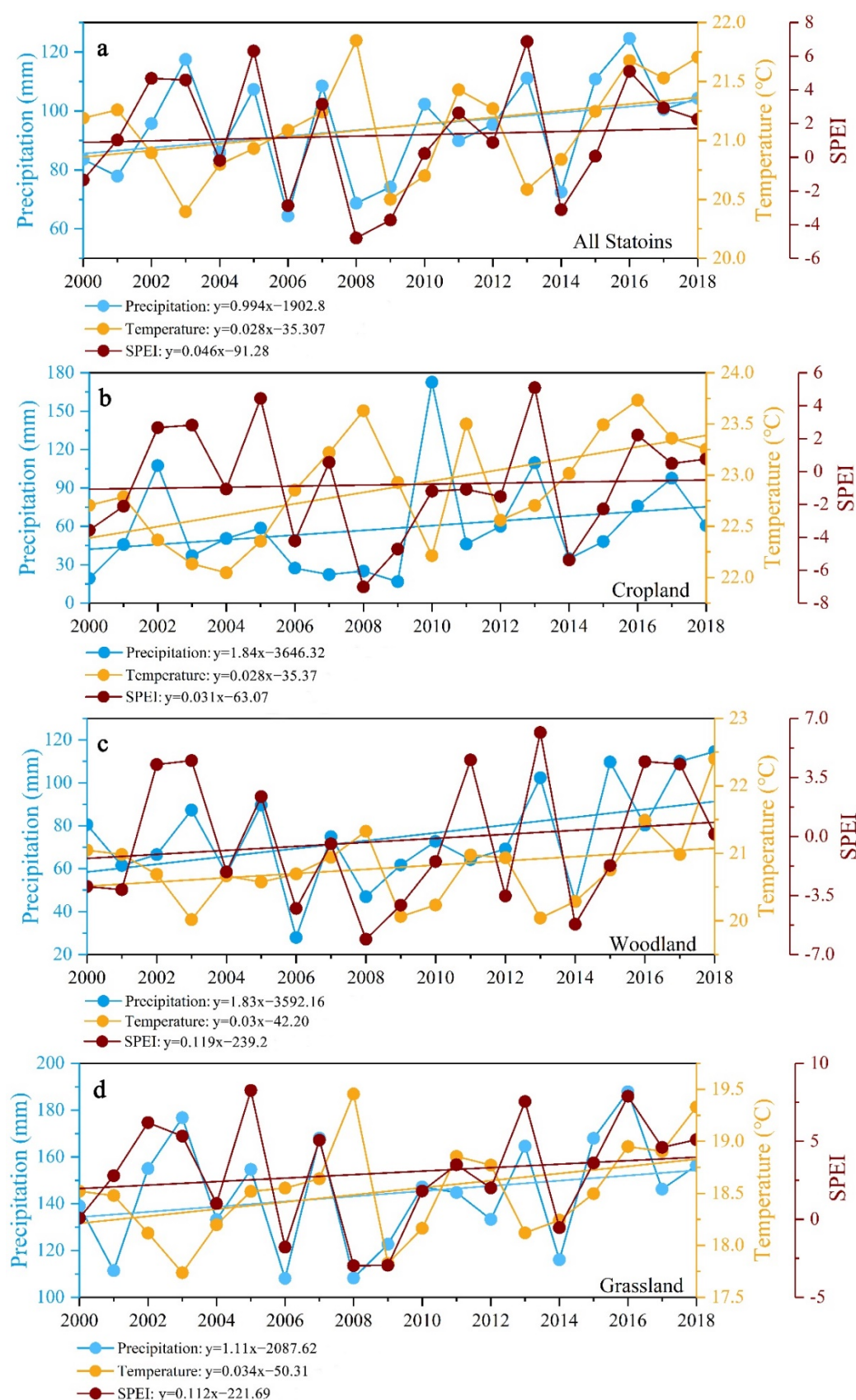


Figure 5. Long-term growing season (May–September) total precipitation, and average mean temperature and SPEI, spatially aggregated over (a) Xinjiang, (b) cropland, (c) woodland and (d) grassland. Comparison was performed based on average values during growing season in the 42 meteorological stations over 2000–2018. The regression lines are drawn for every climate factor and the label shows the corresponding regression equation.

We also used the TerraClimate dataset to analyze the spatial distribution characteristics of different climatic factors (Figure 6). The overall spatial pattern of change rates of precipitation and SPEI were contrary to that of temperature. Precipitation declined significantly in the Ili River Valley, Altay Mountains and the regions to the north, and increased in the Kunlun Mountains, southern Tianshan Mountains and east of the Hami basin. The temperature decreased in the southeastern part of Xinjiang and rose significantly in the northerly regions of Xinjiang and the western border of the Tarim Basin. We can see that SPEI decreased in the Altay Mountains and in the Ili River regions where temperature increased and precipitation decreased. SPEI also increased in the areas where temperature decreased and precipitation increased, for example, the southeast part of Xinjiang and south of the Junggar Basin. Therefore, the changes in SPEI comprehensively reflect the changes in precipitation and temperature. We find that southern Xinjiang has become significantly wetter, and the areas around the Ili River Valley have become drier. The increasing trend in humidity in southern Xinjiang may be affected by the monsoons.

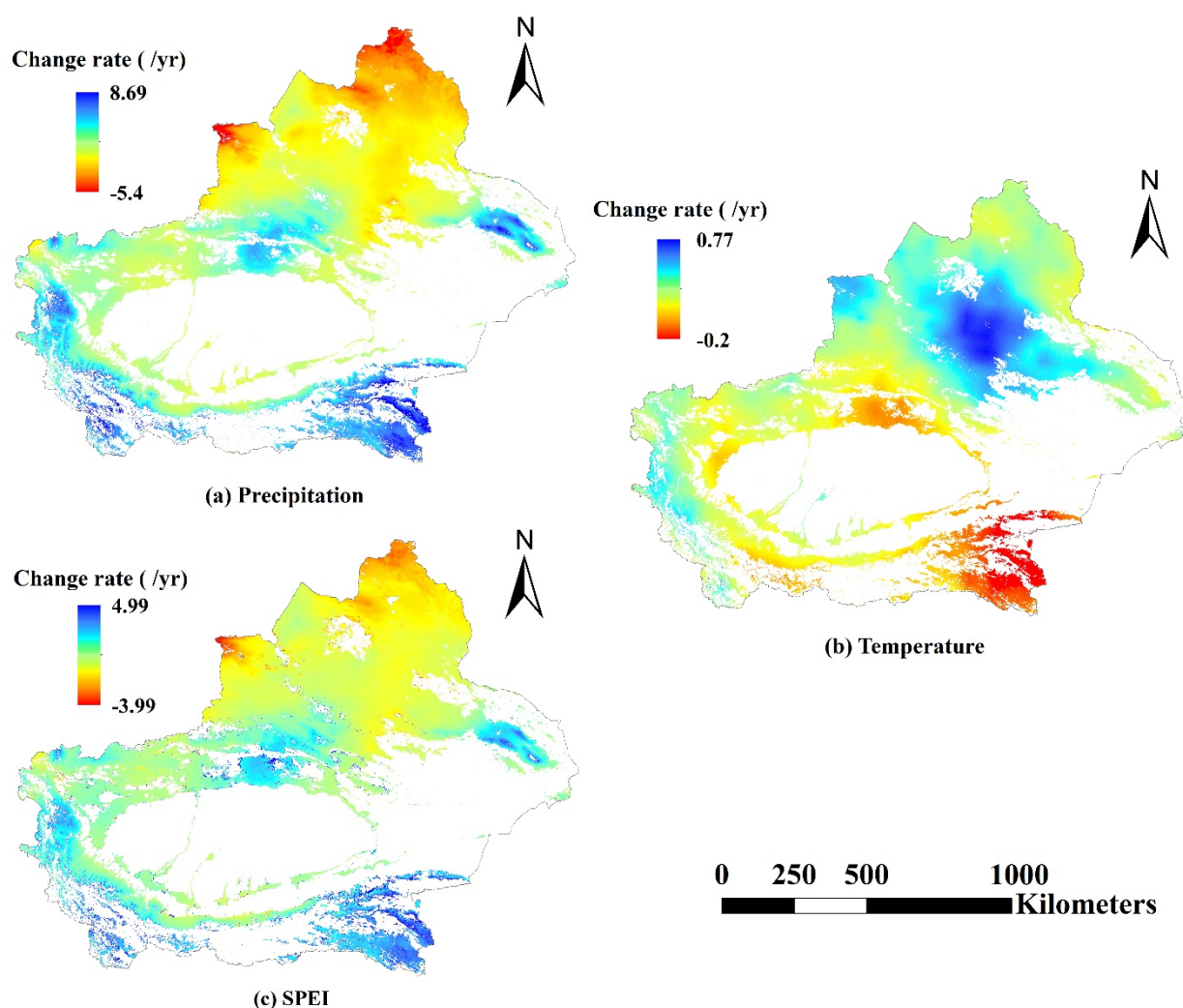


Figure 6. Spatial distribution of climate change rate for May to September of 2000–2019, (a) Change rate of annual precipitation accumulation, (b) Change rate of mean temperature, (c) Change rate of SPEI.

3.3. Response of Vegetation to Climate

We drew scatter plots (Figure 7) and spatial distribution maps (Figure 8) of the correlation between NDVI and climate factors to reveal the reasons for vegetation changes. We comprehensively analyzed and selected some suitable meteorological stations with

different land use types according to the data integrity of meteorological stations and their distance to densely populated areas and other disturbing factors. Meanwhile, we made a 10 km circle buffer zone for every meteorological station and averaged the NDVI values of all pixels within a buffer zone to calculate the representative NDVI. In Figure 7, we can see that NDVI has the highest correlation with SPEI ($R^2 = 0.69$), followed by precipitation ($R^2 = 0.48$), and lowest correlation is with temperature ($R^2 = 0.43$). SPEI has the highest correlation with all three land use types. As for cropland, the contribution of temperature to the growth of cultivated vegetation is more than the precipitation. We found that the R^2 between NDVI and precipitation is 0.2 and it is 0.31 with temperature. As for woodlands and grasslands, NDVI of these two kinds of land use responded more to precipitation than temperature. The R^2 between woodland NDVI and precipitation is 0.42, and 0.12 with temperature. Meanwhile, the R^2 between grassland NDVI and precipitation is 0.44, and 0.104 with temperature. The results revealed that different vegetation responds differently to climate change. The growth of natural vegetation is more dependent on precipitation than artificial (irrigated) vegetation.

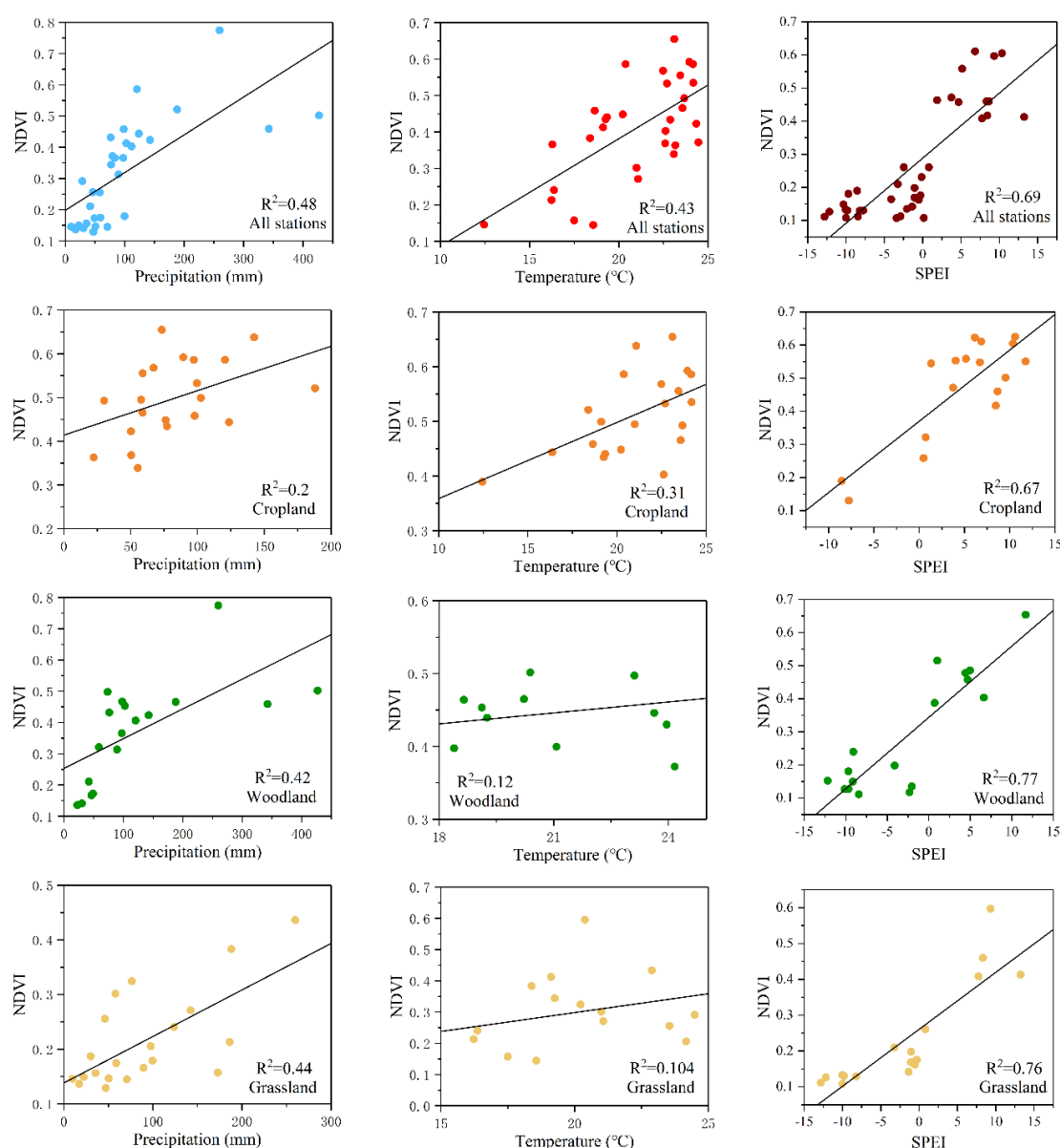


Figure 7. Correlations between the mean value of NDVI of three land use types and the mean annual total precipitation of meteorological stations, the mean annual mean temperature and SPEI during the 2000–2018 growing season in Xinjiang.

The Pearson correlation was calculated for each pixel, which provides a better reflection of the interaction between NDVI and temperature or precipitation for different land use types across locations (Figure 8). Figure 8 shows that the correlation between NDVI and precipitation was strongly positive in the Tianshan Mountains, the mountains in the west of the Junggar Basin and the southwestern part of the Tarim Basin. These areas are mainly grassland and woodland. We found that the correlation between NDVI and temperature was weakly positive and moderately negative in woodland and grassland. However, it was strongly positive in cropland, which is largely spread over the south of the Junggar Basin and around the Hami basin. The spatial correlation patterns of SPEI were similar to precipitation. Meanwhile, we calculated that the proportions of the pixels in which NDVI positively correlated with precipitation, temperature and SPEI were 79.79%, 55.24%, and 88.29%, respectively. In comparison, the proportions of the pixels that NDVI negatively correlated with precipitation, temperature and SPEI were 20.21%, 44.76% and 11.72%, respectively. The results revealed that different climate factors have varied effects on vegetation growth. Moreover, NDVI showed a very high relationship with SPEI, which indicated SPEI performs well in describing the interaction between climate variation and plants growth over the dryland. SPEI reflects the relationship with vegetation growth, and shows that precipitation has a great impact on vegetation growth.

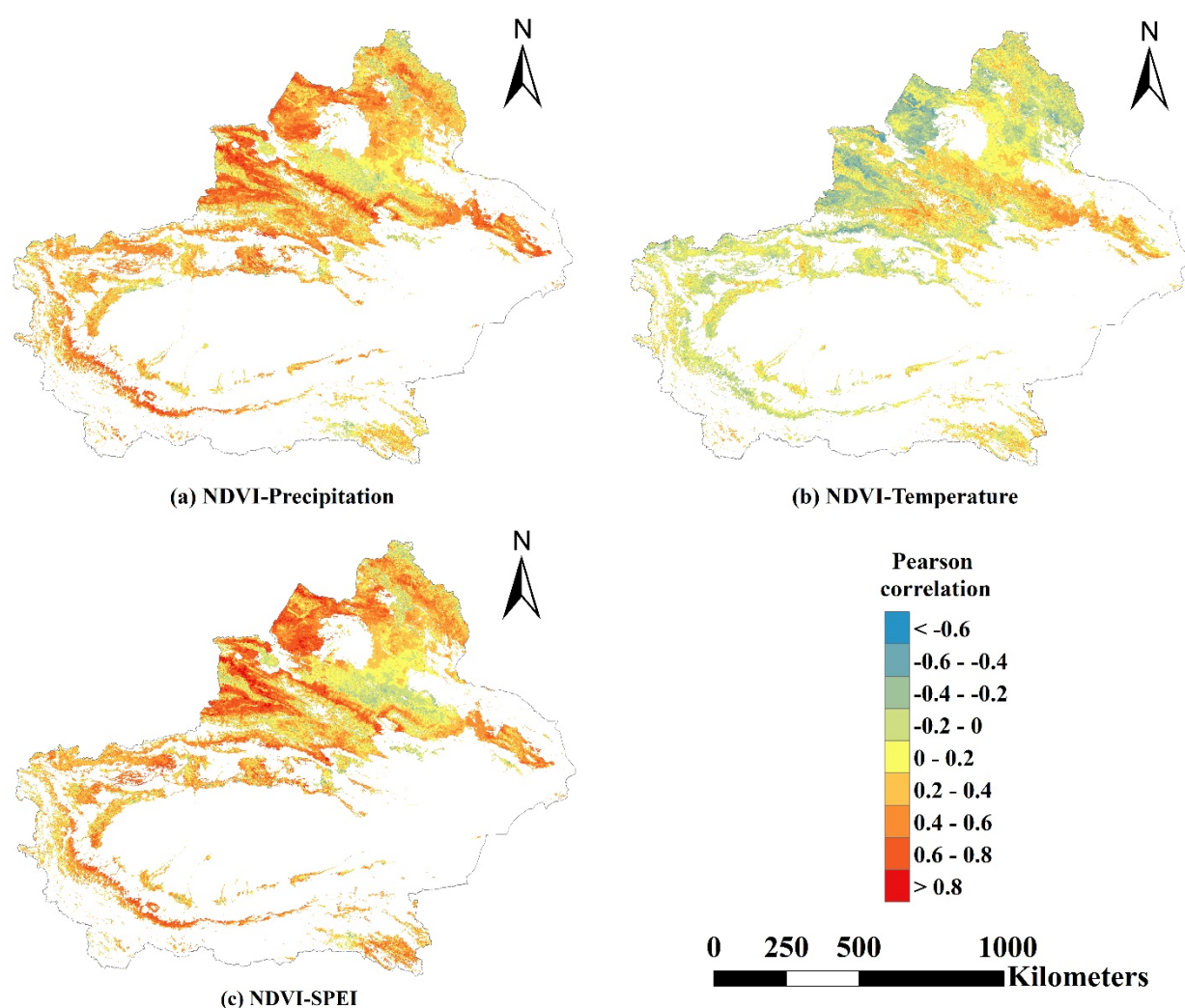


Figure 8. Pearson correlation between the mean value of NDVI during the 2000–2019 growing season and (a) the average annual total precipitation, (b) the average annual mean temperature, and (c) the SPEI of TerraClimate dataset.

4. Discussion

4.1. Analysis of NDVI Change Trends and Effects of Climate Factors to Vegetation

This study revealed the spatial and vegetation-specific NDVI dynamic changes in Xinjiang (Figure 3). The NDVI_{mean} trends showed that 95.35% of Xinjiang has been greening since 2000 and long-term greening is widespread over the province. There were only a few areas with browning. On average, R_{mean} for 2000 to 2019 was 0.0011. This rate is lower than the global estimation (0.00069) during the period 1982–2013 [23]. However, different data sources and study periods may explain the differences.

Variations in environmental conditions caused by climate affect the growth of vegetation [56]. The effect of climatic elements such as precipitation and temperature on vegetation growth is mainly dependent on the characteristics of different environments [57]. The NDVI trends may be influenced by the variations in temperature and precipitation. This research confirms the existing assertions that temperature and precipitation have increased [24]. From the results of the land use types, due to the distinct growth characteristics of various vegetation, the reaction of different plants may be variable in the context of climate change [27].

There has been an obvious growing tendency of NDVI in the edge of the Tarim Basin and Jungar Basin, which are mainly cropland. In order to discuss the responses of NDVI to climate change in depth, we extracted the cropland for two types (rain-fed and irrigated) using the GLC_FCS30 dataset [58], and analysis was respectively conducted over two kinds of cropland. The Figure 9 displays some differences between rain-fed cropland and irrigated cropland. NDVI peaks were observed for rain-fed crops in high SPEI years, in which the precipitation was relatively heavy. The finding was in line with previous research showing that the condition of rain-fed crops highly depended on precipitation [59,60]. As shown in Figure 9, Xinjiang experienced severe drought in 2008 and 2014 when the temperature was high, the precipitation was low and the SPEI was high. In these two years, the extremely low values were observed within the NDVI of rain-fed crops, while irrigated crops did not show the same situation. NDVI of the two types of crop increased during the study period, while the interannual difference of NDVI of rain-fed crops was greater than that of irrigated crops and the crop condition of irrigated was better than rain-fed as a whole. These fully demonstrated that irrigation has significantly alleviated plant water stress and boosted the growth of the average soil moisture, which can in turn promote crop growth, especially in a dry year [61]. Agriculture in Xinjiang is dominated by oasis agriculture, and there are very few rain-fed crops. Therefore, the growth of crops is very dependent on irrigation, especially in arid areas [56]. Because of limited precipitation, overflowing floodwaters and groundwater are also important water sources for crop growth. At the same time, temperature showed a rising trend from 2000 to 2019, and the melting water of Tianshan Mountains increased, which led to an increase in NDVI. Most of the water needed for crop growth was provided by these water sources, making it insensitive to natural rainfall [24]. Among the three types of land use, temperature contributed the most to irrigated cropland NDVI, denoting that the growth of irrigated crops is easily affected by temperature [29].

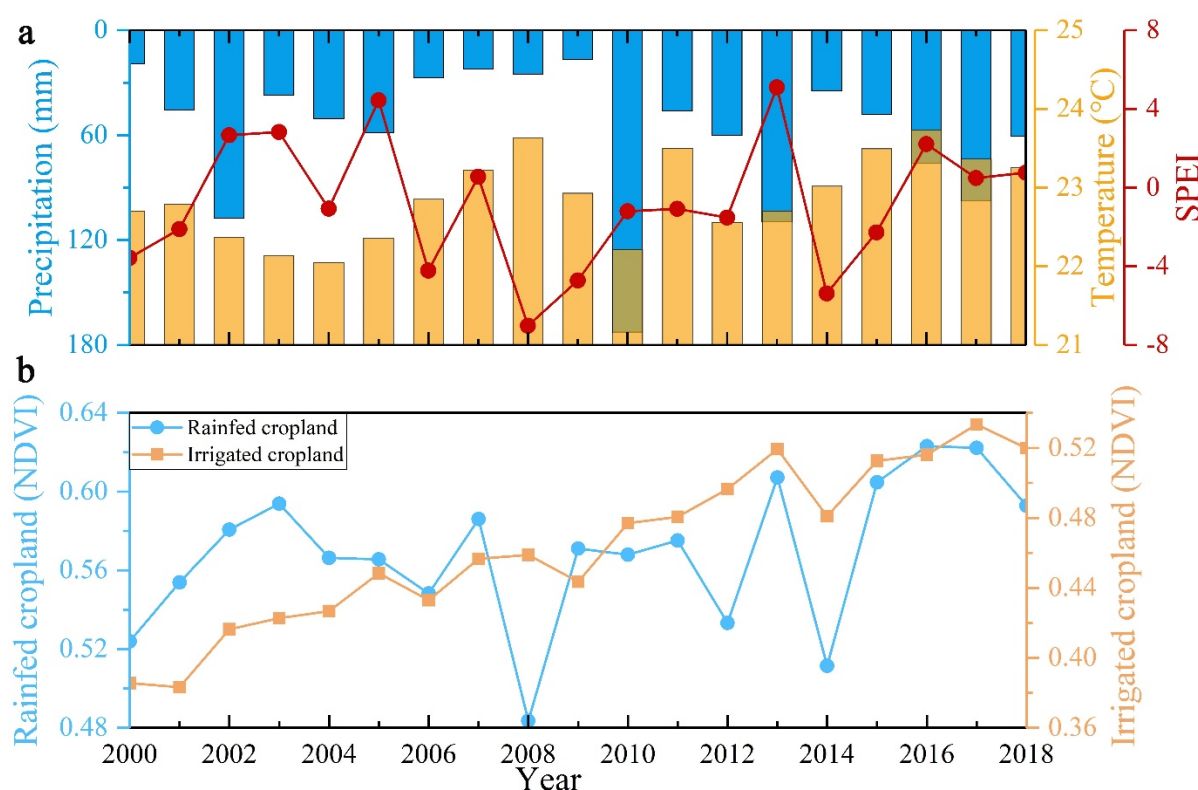


Figure 9. Long-term growing season (May–September) trend of (a) total precipitation, and average mean temperature and SPEI that spatially aggregated over cropland, (b) the average NDVI_{mean} of the grid cells for rain-fed and irrigated cropland.

NDVI of woodland increased at a steady rate, which was faster than grassland and slower than cropland. The natural vegetation is relatively more sensitive to changes in precipitation due to the shortage of water resources [53]. Therefore, woodland is sensitive to changes in precipitation while insensitive to temperate changes in Xinjiang. We can see that most of the woodland areas were greening during 2000–2019 because of increased precipitation during the study period. Mountain vegetation, such as coniferous forests growing on shady slopes depends on rainfall instead of groundwater due to the shallow root system [24]. The incremental precipitation in the plant growing season improves the conditions of plants. In addition, rising temperature will lead to increased snowmelt in mountains, which will increase soil moisture and vegetation growth.

We found the browning areas were mostly distributed in the southern Altai Mountains around the Ili River Valley and some areas along the border of the Tarim Basin. The land use type of these areas is mainly grassland, where the NDVI is more susceptible to precipitation than other vegetation. Meanwhile, the SPEI indicated that drought occurred in these areas during 2000–2019. Therefore, the decrease in precipitation and the increase in evaporation reduced the water available for vegetation, which is an important cause of grassland degradation.

4.2. Effects of Other Factors on Vegetation

The drivers affecting the NDVI changes are both natural and human [62,63]. Although climate is a key factor affecting NDVI, terrain [7], soil attributes [64] and other natural factors cannot be ignored.

Changes in cropping systems have contributed to the increase in NDVI on croplands. Cotton, for instance, has experienced a short, dense, and early cultivation mode based on dense planting, dwarf plants, early emergence and early maturity, which has been beneficial in achieving high and excellent quality yield for cotton in recent years [65].

The degradation in grassland is similar to that in existing studies [43], with certain discrepancies due to inconsistent data sources and research period. The grassland in the Ili River Valley was a relatively severely degraded area. Due to the combined influence of many factors such as climate change, overloading and overgrazing, pests and rodents, and insufficient investment in construction, the situation of grassland degradation has been severe in recent years [66,67].

The increase in woodland NDVI may be the result of major vegetation projects. Since 1977, the government of Xinjiang has attached great importance to forestry, and has actively promoted and strengthened the construction of key forestry projects under the guidance of the ideology of forestry ecological benefit first. Consequently, great progress has been made in forestry development.

The results of our study reflect the long-term vegetation change trend in Xinjiang and its response to climate factors to a certain extent. The observed patterns are helpful in realizing the evolution of the dryland ecosystem in Xinjiang. This may provide new ideas in protecting fragile ecosystems in arid regions such as Xinjiang. For example, the rain-fed vegetation can be a climate change receptor due to high sensitivity to it and the fact that irrigated vegetation shows low sensitivity to climate change, so the two type of vegetation can be mixed-planted. Meanwhile, more detailed measures should be implemented according to the specific situation. In this way, we can better deal with the impact of climate change on the ecological environment. In addition, the findings can further serve as a useful reference and technical support for local adaptive decision-making. The GEE used in this study can make the continuous and rapid observation of vegetation growth come true, which would further facilitate local management of dry-land ecosystems. Better management of dryland ecosystems can enhance grain safety, biological diversity and sustainability under climate change conditions.

5. Conclusions

The study was undertaken to investigate the change in vegetation greenness and its response to climate in Xinjiang from 2000 to 2019 based on the Google Earth Engine platform. The study provides a new idea for ecological protection in arid areas. However, the effects of terrain, soil attributes and other natural factors and human activities on the growth of vegetation cannot be ignored. We need further discoveries in future studies. The main results are as follows:

- (a) The overall NDVI increased during 2000–2019 in Xinjiang, and the NDVI of three kinds of land use (cropland, woodland and grassland) were all in growth trend. The change rate of mean and maximum NDVI were 0.0011 per year and 0.0013 per year, respectively.
- (b) Xinjiang overall experienced warming and wet trends over the past 20 years. SPEI is a good indicator of climate change.
- (c) In arid regions, growth is more dominated by precipitation than temperature for vegetation. These areas commonly have limited water resources because of low precipitation and high evaporation. Overall, the correlation between NDVI and precipitation ($R^2 = 0.48$) is higher than that of temperature ($R^2 = 0.42$). Meanwhile, natural vegetation is more sensitive to climate change than artificial vegetation.

Author Contributions: Conceptualization, J.X., Y.W. and Z.S.; methodology, J.X. and H.T.; software, J.X. and Y.W.; validation, J.X.; formal analysis, J.X. and Y.W.; investigation, J.X. and J.P.; data curation, N.W. and D.L.; writing—original draft preparation, J.X., Y.W. and J.P.; writing—review and editing, J.X., H.T. and A.B.; visualization, J.X. and H.T.; supervision, Z.S.; funding acquisition, Z.S. All authors have read and agreed to the published version of the manuscript.

Funding: This research was funded by the National Key Research and Development Program (2018YFE0107000), and Ten-thousand Talents Plan of Zhejiang Province (2019R52004).

Institutional Review Board Statement: Not applicable.

Informed Consent Statement: Not applicable.

Data Availability Statement: Not applicable.

Conflicts of Interest: The authors declare no conflict of interest.

Reference

1. Parmesan, C.; Yohe, G. A globally coherent fingerprint of climate change impacts across natural systems. *Nature* **2003**, *421*, 37–42.
2. Forzieri, G.; Alkama, R.; Miralles, D.G.; Cescatti, A. Satellites reveal contrasting responses of regional climate to the widespread greening of Earth. *Science* **2017**, *365*, 1180–1184.
3. Ballantyne, A.; Smith, W.; Anderegg, W.; Kauppi, P.; Sarmiento, J.; Tans, P.; Shevliakova, E.; Pan, Y.; Poulter, B.; Anav, A.; et al. Accelerating net terrestrial carbon uptake during the warming hiatus due to reduced respiration. *Nat. Clim. Change* **2017**, *7*, 148–152. <https://doi.org/10.1038/nclimate3204>.
4. Piao, S.; Yin, G.; Tan, J.; Cheng, L.; Huang, M.; Li, Y.; Liu, R.; Mao, J.; Myneni, R.B.; Peng, S.; et al. Detection and attribution of vegetation greening trend in China over the last 30 years. *Glob. Change Biol.* **2015**, *21*, 1601–1609. <https://doi.org/10.1111/gcb.12795>.
5. Mao, J.; Shi, X.; Thornton, P.; Hoffman, F.; Zhu, Z.; Myneni, R. Global Latitudinal-Asymmetric Vegetation Growth Trends and Their Driving Mechanisms: 1982–2009. *Remote Sens.* **2013**, *5*, 1484–1497. <https://doi.org/10.3390/rs5031484>.
6. Xu, L.; Myneni, R.B.; Chapin III, F.S.; Callaghan, T.V.; Pinzon, J.E.; Tucker, C.J.; Zhu, Z.; Bi, J.; Ciais, P.; Tømmervik, H.; et al. Temperature and vegetation seasonality diminishment over northern lands. *Nat. Clim. Change* **2013**, *3*, 581–586. <https://doi.org/10.1038/nclimate1836>.
7. Teng, H.; Luo, Z.; Chang, J.; Shi, Z.; Chen, S.; Zhou, Y.; Ciais, P.; Tian, H. Climate change-induced greening on the Tibetan Plateau modulated by mountainous characteristics. *Environ. Res. Lett.* **2021**, *16*. <https://doi.org/10.1088/1748-9326/abfeeb>.
8. Lian, X.; Piao, S.; Chen, A.; Huntingford, C.; Fu, B.; Li, L.Z.X.; Huang, J.; Sheffield, J.; Berg, A.M.; Keenan, T.F.; et al. Multifaceted characteristics of dryland aridity changes in a warming world. *Nat. Rev. Earth Environ.* **2021**, *2*, 232–250. <https://doi.org/10.1038/s43017-021-00144-0>.
9. He, B.; Wang, S.; Guo, L.; Wu, X. Aridity change and its correlation with greening over drylands. *Agric. For. Meteorol.* **2019**, *278*. <https://doi.org/10.1016/j.agrformet.2019.107663>.
10. Safriel, U.; Adeel, Z.; Niemeijer, D.; Puigdefabregas, J.; White, R.; Lal, R.; Winslow, M.; Ziedler, J.; Prince, S.; Archer, E.C. *King Chapter 22: Dryland systems Millennium Ecosystem Assessment. Ecosystems and Human Well-Being*; World Resources Institute: Washington, DC, USA, 2005; pp. 623–662.
11. Middleton, N.J.; Sternberg, T. Climate hazards in drylands: A review. *Earth Sci. Rev.* **2013**, *126*, 48–57. <https://doi.org/10.1016/j.earscirev.2013.07.008>.
12. Smith, W.K.; Dannenberg, M.P.; Yan, D.; Herrmann, S.; Barnes, M.L.; Barron-Gafford, G.A.; Biederman, J.A.; Ferrenberg, S.; Fox, A.M.; Hudson, A.; et al. Remote sensing of dryland ecosystem structure and function: Progress, challenges, and opportunities. *Remote Sens. Environ.* **2019**, *233*. <https://doi.org/10.1016/j.rse.2019.111401>.
13. Tucker, C.J. Red and photographic infrared linear combinations for monitoring vegetation. *Remote Sens. Environ.* **1979**, *8*, 127–150.
14. Huete, A.; Didan, K.; Miura, T.; Rodriguez, E.P.; Gao, X.; Ferreira, L.G. Overview of the radiometric and biophysical performance of the MODIS vegetation indices. *Remote Sens. Environ.* **2002**, *83*, 195–213.
15. Beck, H.E.; McVicar, T.R.; van Dijk, A.I.J.M.; Schellekens, J.; de Jeu, R.A.M.; Bruijnzeel, L.A. Global evaluation of four AVHRR–NDVI data sets: Intercomparison and assessment against Landsat imagery. *Remote Sens. Environ.* **2011**, *115*, 2547–2563. <https://doi.org/10.1016/j.rse.2011.05.012>.
16. Thompson, J.A.; Paull, D.J. Assessing spatial and temporal patterns in land surface phenology for the Australian Alps (2000–2014). *Remote Sens. Environ.* **2017**, *199*, 1–13. <https://doi.org/10.1016/j.rse.2017.06.032>.
17. Piao, S.; Liu, Q.; Chen, A.; Janssens, I.A.; Fu, Y.; Dai, J.; Liu, L.; Lian, X.; Shen, M.; Zhu, X. Plant phenology and global climate change: Current progresses and challenges. *Glob. Change Biol.* **2019**, *25*, 1922–1940. <https://doi.org/10.1111/gcb.14619>.
18. Gamon, J.A.; Field, C.B.; Goulden, M.L.; Griffin, K.L.; Hartley, A.E.; Joel, G.; Penuelas, J.; Valentini, R. Relationships Between NDVI, Canopy Structure, and Photosynthesis in Three Californian Vegetation Types. *Ecol. Appl.* **1995**, *5*, 28–41.
19. Anderson, G.L.; Hanson, J.D.; Haas, R.H. Evaluating landsat thematic mapper derived vegetation indices for estimating above-ground biomass on semiarid rangelands. *Remote Sens. Environ.* **1993**, *45*, 165–175.
20. Pettorelli, N.; Vik, J.O.; Mysterud, A.; Gaillard, J.M.; Tucker, C.J.; Stenseth, N.C. Using the satellite-derived NDVI to assess ecological responses to environmental change. *Trends Ecol. Evol.* **2005**, *20*, 503–510. <https://doi.org/10.1016/j.tree.2005.05.011>.
21. Jeong, S.J.; Ho, C.H.; Gim, H.J.; Brown, M.E. Phenology shifts at start vs. end of growing season in temperate vegetation over the Northern Hemisphere for the period 1982–2008. *Glob. Change Biol.* **2011**, *17*, 2385–2399. doi:10.1111/j.1365-2486.2011.02397.x.
22. Piao, S.L.; Fang, J.Y.; Zhou, L.M.; Guo, Q.H.; Henderson, M.; Ji, W.; Li, Y.; Tao, S. Interannual variations of monthly and seasonal normalized difference vegetation index (NDVI) in China from 1982 to 1999. *J. Geophys. Res. Atmos.* **2003**, *108*, 4401. <https://doi.org/10.1029/2002JD002848>.

23. Pan, N.; Feng, X.; Fu, B.; Wang, S.; Ji, F.; Pan, S. Increasing global vegetation browning hidden in overall vegetation greening: Insights from time-varying trends. *Remote Sens. Environ.* **2018**, *214*, 59–72. <https://doi.org/10.1016/j.rse.2018.05.018>.
24. Liang, S.; Yi, Q.; Liu, J. Vegetation dynamics and responses to recent climate change in Xinjiang using leaf area index as an indicator. *Ecol. Indic.* **2015**, *58*, 64–76. <https://doi.org/10.1016/j.ecolind.2015.05.036>.
25. Myers-Smith, I.H.; Kerby, J.T.; Phoenix, G.K.; Bjerke, J.W.; Epstein, H.E.; Assmann, J.J.; John, C.; Andreu-Hayles, L.; Angers-Blondin, S.; Beck, P.S.A.; et al. Complexity revealed in the greening of the Arctic. *Nat. Clim. Change* **2020**, *10*, 106–117. <https://doi.org/10.1038/s41558-019-0688-1>.
26. Fensholt, R.; Langanke, T.; Rasmussen, K.; Reenberg, A.; Prince, S.D.; Tucker, C.; Scholes, R.J.; Le, Q.B.; Bondeau, A.; Eastman, R.; et al. Greenness in semi-arid areas across the globe 1981–2007—An Earth Observing Satellite based analysis of trends and drivers. *Remote Sens. Environ.* **2012**, *121*, 144–158. <https://doi.org/10.1016/j.rse.2012.01.017>.
27. Andela, N.; Liu, Y.Y.; van Dijk, A.I.J.M.; de Jeu, R.A.M.; McVicar, T.R. Global changes in dryland vegetation dynamics (1988–2008) assessed by satellite remote sensing: Comparing a new passive microwave vegetation density record with reflective greenness data. *Biogeosciences* **2013**, *10*, 6657–6676. <https://doi.org/10.5194/bg-10-6657-2013>.
28. Huang, J.; Yu, H.; Guan, X.; Wang, G.; Guo, R. Accelerated dryland expansion under climate change. *Nat. Clim. Change* **2015**, *6*, 166–171. <https://doi.org/10.1038/nclimate2837>.
29. Nemani, R.R.; Keeling, C.D.; Hashimoto, H.; Jolly, W.M.; Piper, S.C.; Tucker, C.J.; Myneni, R.B.; Running, S.W. Climate-Driven Increases in Global Terrestrial Net Primary Production from 1982 to 1999. *Science* **2003**, *300*, 1560–1563.
30. Fensholt, R.; Rasmussen, K.; Nielsen, T.T.; Mbow, C. Evaluation of earth observation based long term vegetation trends—Inter-comparing NDVI time series trend analysis consistency of Sahel from AVHRR GIMMS, Terra MODIS and SPOT VGT data. *Remote Sens. Environ.* **2009**, *113*, 1886–1898. <https://doi.org/10.1016/j.rse.2009.04.004>.
31. Justice, C.; Belward, A.; Morisette, J.; Lewis, P.; Privette, J.; Baret, F. Developments in the ‘validation’ of satellite sensor products for the study of the land surface. *Int. J. Remote Sens.* **2010**, *21*, 3383–3390. <https://doi.org/10.1080/014311600750020000>.
32. Zhu, Y.X.; Zu, J.X.; Zhang, J.Y.; Che, B.; Tang, Z.; Cong, N.; Li, J.X.; Chen, N. Performance evaluation of GIMMS NDVI based on MODIS NDVI and SPOT NDVI data. *Chin. J. Appl. Ecol.* **2019**, *30*, 536–544. (In Chinese)
33. Zhang, G.; Zhang, Y.; Dong, J.; Xiao, X. Green-up dates in the Tibetan Plateau have continuously advanced from 1982 to 2011. *Proc. Natl. Acad. Sci. USA* **2013**, *110*, 4309–4314. <https://doi.org/10.1073/pnas.1210423110>.
34. Song, F.Q.; Kang, M.Y.; Yang, P.; Chen, Y.R.; Liu, Y.; Xing, K.X. Comparison and validation of GIMMS, SPOT-VGT and MODIS global NDVI products in the Loess Plateau of northern Shaanxi Province, northwestern China. *J. Beijing For. Univ.* **2010**, *32*, 72–80. <https://doi.org/10.13332/j.1000-1522.2010.04.031>. (In Chinese)
35. Luo, N.N.; Mao, D.H.; Wen, B.L.; Liu, X.T. Climate Change Affected Vegetation Dynamics in the Northern Xinjiang of China: Evaluation by SPEI and NDVI. *Land* **2020**, *9*, 90. <https://doi.org/10.3390/land9030090>.
36. Park, H.; Jeong, S.; Penuelas, J. Accelerated rate of vegetation green-up related to warming at northern high latitudes. *Glob. Change Biol.* **2020**, *26*, 6190–6202. <https://doi.org/10.1111/gcb.15322>.
37. Vicente-Serrano, S.M.; Van der Schrier, G.; Begueria, S.; Azorin-Molina, C.; Lopez-Moreno, J.-I. Contribution of precipitation and reference evapotranspiration to drought indices under different climates. *J. Hydrol.* **2015**, *526*, 42–54. <https://doi.org/10.1016/j.jhydrol.2014.11.025>.
38. Bushra, N.; Rohli, R.V.; Lam, N.S.N.; Zou, L.; Mostafiz, R.B.; Mihunov, V. The relationship between the Normalized Difference Vegetation Index and drought indices in the South Central United States. *Nat. Hazards* **2019**, *96*, 791–808. <https://doi.org/10.1007/s11069-019-03569-5>.
39. Bunting, E.L.; Munson, S.M.; Bradford, J.B. Assessing plant production responses to climate across water-limited regions using Google Earth Engine. *Remote Sens. Environ.* **2019**, *233*. <https://doi.org/10.1016/j.rse.2019.111379>.
40. Jia, J.H.; Liu, H.Y.; Lin, Z.S. Multi-time scale changes of vegetation NPP in six provinces of northwest China and their responses to climate change. *Acta Ecol. Sin.* **2019**, *39*, 5058–5069. (In Chinese)
41. Yao, J.; Hu, W.; Chen, Y.; Huo, W.; Zhao, Y.; Mao, W.; Yang, Q. Hydro-climatic changes and their impacts on vegetation in Xinjiang, Central Asia. *Sci. Total Environ.* **2019**, *660*, 724–732. <https://doi.org/10.1016/j.scitotenv.2019.01.084>.
42. Li, Q.; Chen, Y.; Shen, Y.; Li, X.; Xu, J. Spatial and temporal trends of climate change in Xinjiang, China. *J. Geogr. Sci.* **2011**, *21*, 1007–1018. <https://doi.org/10.1007/s11442-011-0896-8>.
43. Zhang, F.; Wang, C.; Wang, Z.-H. Response of Natural Vegetation to Climate in Dryland Ecosystems: A Comparative Study between Xinjiang and Arizona. *Remote Sens.* **2020**, *12*, 3567. <https://doi.org/10.3390/rs12213567>.
44. Xu, Y.; Yang, J.; Chen, Y. NDVI-based vegetation responses to climate change in an arid area of China. *Theor. Appl. Climatol.* **2016**, *126*, 213–222.
45. Zhang, Q.; Li, J.; Singh, V.P.; Bai, Y. SPI-based evaluation of drought events in Xinjiang, China. *Nat. Hazards* **2012**, *64*, 481–492. <https://doi.org/10.1007/s11069-012-0251-0>.
46. Zhou, L.; Tucker, C.J.; Kaufmann, R.K.; Slayback, D.; Shabanov, N.V.; Myneni, R.B. Variations in northern vegetation activity inferred from satellite data of vegetation index during 1981 to 1999. *J. Geophys. Res. Atmos.* **2001**, *106*, 20069–20083. <https://doi.org/10.1029/2000jd000115>.
47. Liu, Q.; Fu, Y.H.; Zeng, Z.; Huang, M.; Li, X.; Piao, S. Temperature, precipitation, and insolation effects on autumn vegetation phenology in temperate China. *Glob. Change Biol.* **2016**, *22*, 644–655. <https://doi.org/10.1111/gcb.13081>.
48. Abatzoglou, J.T.; Dobrowski, S.Z.; Parks, S.A.; Hegewisch, K.C. Data Descriptor: Terraclimate, a high-resolution global dataset of monthly climate and climatic water balance from 1958–2015. *Sci. Data* **2018**, *5*, 170191. <https://doi.org/10.1038/sdata.2017.191>.

49. Vicente-Serrano, S.M.; Beguería, S.; López-Moreno, J.I. A Multiscalar Drought Index Sensitive to Global Warming: The Standardized Precipitation Evapotranspiration Index. *J. Clim.* **2010**, *23*, 1696–1718. <https://doi.org/10.1175/2009jcli2909.1>.
50. Chinese Academy of Meteorological Sciences. *Classification of Meteorological Drought*; GBT 20481-2006; China Standards Press: Beijing, China, 2006. (In Chinese)
51. Zhang, J.H.; Feng, Z.M.; Jiang, L.G. Progress on studies of land use/land cover classification systems. *Resour. Sci.* **2010**, *33*, 1195–1203. (In Chinese)
52. MathWorks, Statistics and Machine Learning Toolbox™ User's Guide. **2019**. Available online: <https://kr.mathworks.com/> (accessed on 5 August 2020).
53. Zhou, W.; Yang, H.; Huang, L.; Chen, C.; Lin, X.; Hu, Z.; Li, J. Grassland degradation remote sensing monitoring and driving factors quantitative assessment in China from 1982 to 2010. *Ecol. Indic.* **2017**, *83*, 303–313. <https://doi.org/10.1016/j.ecolind.2017.08.019>.
54. Xinjiang Has Been Hit by a Drought Rarely Seen in History. Available online: http://www.gov.cn/jrzq/2008-07/24/content_1055232.htm (accessed on 24 July 2008).
55. The Xinjiang Corps Suffered a Direct Loss of More than 1.6 Billion Yuan Due to a Rare Drought since Its Founding. Available online: <http://politics.people.com.cn/n/2014/0813/c70731-25459519.html> (accessed on 13 August 2014).
56. Xu, Y.; Xiao, F.; Yu, L. Review of spatio-temporal distribution of net primary productivity in forest ecosystem and its responses to climate change in China. *Acta Ecol. Sin.* **2020**, *40*, 4710–4723. (In Chinese)
57. Kun, X.; Zhang, J.; Lv, X. Spatio-temporal change of marshes NDVI and its response to climate change in the Qinghai-Tibet Plateau. *Acta Ecol. Sin.* **2020**, *40*, 6259–6268. (In Chinese)
58. Liu, L.Y.; Zhang, X.; Chen, X.D.; Gao, Y.; Mi, J. GLC_FCS30: Global Land-Cover Product with Fine Classification System at 30 m Using Time-Series Landsat Imagery (Version v1). 2020. Available online: <http://data.casearth.cn/sdo/detail/6123651428a58f70c2a51e47> (accessed on 23 August 2021).
59. Zheng, H.W.; Wu, B.F.; Zou, W.T.; Yan, N.N.; Zhang, M. Performance comparison of crop condition assessments in irrigated and rain-fed areas: A case study in Nebraska. *J. Remote Sens.* **2015**, *19*, 560–567. <https://doi.org/10.11834/jrs.20154144>. (In Chinese)
60. Islam, M.A.; Obour, A.K.; Krall, J.M.; Cecil, J.T.; Nachtman, J.J. Performance of turfgrass under supplemental irrigation and rain-fed conditions in the Central Great Plains of USA. *Grassl. Sci.* **2013**, *59*, 111–119. <https://doi.org/10.1111/grs.12018>.
61. Wang, C. Landscape phenology and soil moisture dynamics influenced by irrigation in a desert urban environment. In Proceedings of the 54th International Conference of the Architectural Science Association: Auckland, New Zealand, 25–28 November 2020; pp. 670–679.
62. Zhu, Z.; Piao, S.; Myneni, R.B.; Huang, M.; Zeng, Z.; Canadell, J.G.; Ciais, P.; Sitch, S.; Friedlingstein, P.; Arneeth, A.; et al. Greening of the Earth and its drivers. *Nat. Clim. Change* **2016**, *6*, 791–795. <https://doi.org/10.1038/nclimate3004>.
63. Li, M.H.; Du, J.K.; Li, R.J.; Wu, S.Y.; Wang, S.S. Global Vegetation Change and Its Relationship with Precipitation and Temperature Based on GLASS-LAI in 1982–2015. *Sci. Geogr. Sin.* **2020**, *40*, 823–832. <https://doi.org/10.13249/j.cnki.sgs.2020.05.017>. (In Chinese)
64. Luo, Y.; Peng, Q.; Li, K.; Gong, Y.; Liu, Y.; Han, W. Patterns of nitrogen and phosphorus stoichiometry among leaf, stem and root of desert plants and responses to climate and soil factors in Xinjiang, China. *Catena* **2021**, *199*. <https://doi.org/10.1016/j.catena.2020.105100>.
65. Lou, S.W.; Dong, H.Z.; Tian, X.L.; Tian, L. The “Short, Dense and Early” Cultivation of Cotton in Xinjiang: History, Current Situation and Prospect. *Sci. Agric. Sin.* **2021**, *54*, 720–732. <https://doi.org/10.3864/j.issn.0578-1752.2021.04.005>. (In Chinese)
66. Liu, F.; Zhang, H.Q.; Dong, G.L. Vegetation Dynamics and Precipitation Sensitivity in Yili Valley Grassland. *Resour. Sci.* **2014**, *36*, 1724–1731. (In Chinese)
67. Qiao, M.; Feng, Y. Ecological investigation and restoration strategies of spring and autumn pastures in Yili River Valley. *Chin. J. Appl. Ecol.* **2007**, *4*, 528–532. (In Chinese)